JOURNAL OF THERMOPHYSICS AND HEAT TRANSFER
Vol. 24, No. 2, April–June 2010

Solidification in a Continuous Medium with Periodically Distributed Two-Dimensional Circular Pores

B. Zhang, T. Kim,* and T. J. Lu
Xi'an Jiaotong University, 710049 Xi'an People's Republic of China

DOI: 10.2514/1.45937

This paper demonstrates that the temporal variation of solidification interface in a continuous medium containing periodically distributed two-dimensional circular pores can be analytically predicted. Experiments using distilled water as the continuous medium to be solidified (frozen) are conducted to validate the model predictions for two selected porosities: $\varepsilon = 0$ and 0.5. Numerical simulations using the method of finite elements are also carried out to further explore the effect of topological anisotropy associated with pore arrangement on the effective thermal conductivity of the porous medium. The analytical solution well predicts the general trend of the solidification interface with a systematic deviation (underestimation). Such agreement nonetheless suggests that the delay of solidification is mainly caused by the reduction of the bulk thermal conductivity due to the presence of low-conducting pores, as this is the sole mechanism accounted for by the analytical model for solidification in a porous medium.

Nomenclature

c_p	=	specific heat of continuous medium, J/(kg K)
H	=	total thickness of melt along the direction of solidification, m
h_{nc}	=	natural convection heat transfer coefficient, W/(m^2 K)
k_c	=	thermal conductivity of continuous medium, W/(mK)
k_e	=	effective thermal conductivity of bulk medium, W/(mK)
k_p	=	thermal conductivity of discrete pore, W/(mK)
L	=	latent heat, J/kg
L_x, L_y	=	length of simulated domain along x and y axes, m
q''	=	heat flux though solidified layer, W/m
S	=	thickness of solidified layer, m
T_m	=	liquid phase temperature, K
T_s, T_l	=	solid and liquid phase temperatures, K
T_0	=	cooling temperature at $x = 0$, K
t	=	time, s
x	=	coordinate coinciding with solidification direction
α_c	=	thermal diffusivity of continuous medium, m^2/s
α_e	=	effective thermal diffusivity of bulk medium, m^2/s
α_p	=	thermal diffusivity of discrete pore, m^2/s
α_s	=	solid phase thermal diffusivity of continuous medium, m^2/s
ε	=	porosity
λ	=	constant defined by Eq. (2)
ξ	=	nondimensional solidification front, S/H
ρ_e	=	effective density of porous materials, kg/m^3
ρ_c	=	density of continuous medium, kg/m^3
ρ_p	=	density of discrete pore, kg/m^3
τ	=	nondimensional time, $\alpha_s t/H^2$
τ_1, τ_2	=	time constants, s
φ	=	yaw angle, deg
χ	=	nondimensional position, x/H

I. Introduction

PHASE change occurring during solidification (or melting), generally known as the *Stefan problem*, is associated with many practical applications such as castings, welding, heat treatment, thermal energy storage, and freezing or thawing of soils and foods [1–4]. Despite the importance of Stefan or Stefan-type problems and the large amount of efforts devoted to solving these problems, analytical (exact) solutions are still limited to a few idealized situations, due to the mathematical complexities in Stefan problems, including the moving boundaries (interfaces) whose locations are essentially unknown. A comprehensive review of the existing analytical solutions can be found in Carslaw and Jaeger [5]. On the other hand, a variety of approximate methods, including the heat balance integral [6], moving heat source [7], and perturbation [8] have been proposed to simplify the problems.

Previous efforts of estimating the evolution in time of a phase interface have mainly dealt with the solidification (or melting) in *homogeneous* (continuous) materials. However, solidification (or melting) in *heterogeneous* materials containing more than one discrete material with distinctive thermal conductivities is commonly encountered in engineering applications. Recently, an analytical solution capable of predicting the advancement of solidification interface in a continuous medium containing randomly distributed nonconducting pores has been reported [9,10]. The analytical model was successfully implemented to estimate the solidification interface during the fabrication of closed-cell metallic foams via the direct foaming route. To account for the inclusion of the nonconducting pores into the continuous medium, the bulk thermal conductivity in the classical Neumann solution was taken as a function of porosity (void fraction) of the pores. In the present study, distilled water simulates the metallic melt to be solidified and pores serve as the hydrogen bubbles formed, with a large thermal-conductivity ratio between the two media. A further simplification has been made by assuming that the hydrogen bubbles are two-dimensional (2-D). The proposed study is expected to provide physical insight into the key factors governing the solidification behavior of a continuous medium (melt or distilled water) containing a certain amount of low-conducting pores.

Particularly, this study aims to demonstrate the applicability of the aforementioned analytical model [9,10] to a particular case in which low-conducting 2-D circular pores are *periodically* distributed in a continuous medium. To validate the model, experiments using distilled water as the continuous medium to be solidified (frozen) are conducted for two selected porosities: $\varepsilon = 0$ and 0.5. Furthermore, numerical simulations using the finite element method are carried out to account for the topological anisotropy associated with the periodic distribution of the circular pores. The solutions of the present study are limited to periodically distributed 2-D circular pores that have a smaller thermal conductivity than that of the host continuous medium.

Received 11 June 2009; revision received 27 November 2009; accepted for publication 5 December 2009. Copyright © 2009 by the American Institute of Aeronautics and Astronautics, Inc. All rights reserved. Copies of this paper may be made for personal or internal use, on condition that the copier pay the $10.00 per-copy fee to the Copyright Clearance Center, Inc., 222 Rosewood Drive, Danvers, MA 01923; include the code 0887-8722/10 and $10.00 in correspondence with the CCC.

*Ministry of Education Key Laboratory for Strength and Vibration; tongbeum@gmail.com.

II. Modified Neumann's Solution for Nonconducting Pore Inclusions

A. Solidification Interface in a Continuous (Dense) Material

Regarding the solidification of continuous media, an analytical solution exists for a classical but fundamental problem: namely, the so-called Neumann's solution for Stefan or Stefan-type problems. The problem is described as follows. One side of the liquid phase as a continuous medium with a total thickness of H, initially at temperature T_m, is suddenly exposed to temperature $T_0 (T_0 < T_m)$, which is below the freezing temperature at time $t > 0$, so that the solidification takes place from $x = 0$, as illustrated in Fig. 1. When the wall temperature at $x = 0$ is dropped below T_m, a portion of the internal heat is liberated, triggering the onset of solidification along the x axis (assuming one-dimensional solidification).

Solidification is a complex process involving many factors due to 1) mathematical complexity of multidimensional transient heat transfer with a moving boundary; 2) dependence of physical properties on temperature, time, and space; and 3) various physical and chemical reactions occurring during the solidification process, either endothermic or exothermic, generating additional heat. In general, to simplify the problem, all of the relevant physical properties of the material (in either liquid or solid phase) such as the latent heat L, thermal conductivity k_s, diffusivity α_s, and specific heat at constant pressure c_p are assumed to be invariant in temperature, time, and space.

Let the interface separating the liquid phase and the solid phase be represented by $S(t)$ (see Fig. 1). Neumann's solution for the normalized interface location x has the form of [5]

$$\xi = S(t)/H = 2\lambda\sqrt{\tau_s} \tag{1}$$

where τ_s is a nondimensional time defined as $\tau_s = \alpha_s t/H^2$, and λ is the positive root of the following transcendental equation:

$$\lambda\sqrt{\pi}\exp(\lambda^2)\mathrm{erf}(\lambda) = Ste \tag{2}$$

Here, $\mathrm{erf}(\lambda)$ is the Gaussian error function defined as

$$\mathrm{erf}\,(\lambda) = \frac{2}{\sqrt{\pi}}\int_0^{\lambda} e^{-V^2}\,\mathrm{d}V \tag{3}$$

For convenience, $Ste = c_p(T_m - T_0)/L$, representing the ratio of sensible heat to total latent heat in the process of solidification, is introduced and called the Stefan number. When $Ste \to 0$ (i.e., the cooling temperature is equal to the liquid temperature), $\lambda = 0$, indicating that no solidification has taken place.

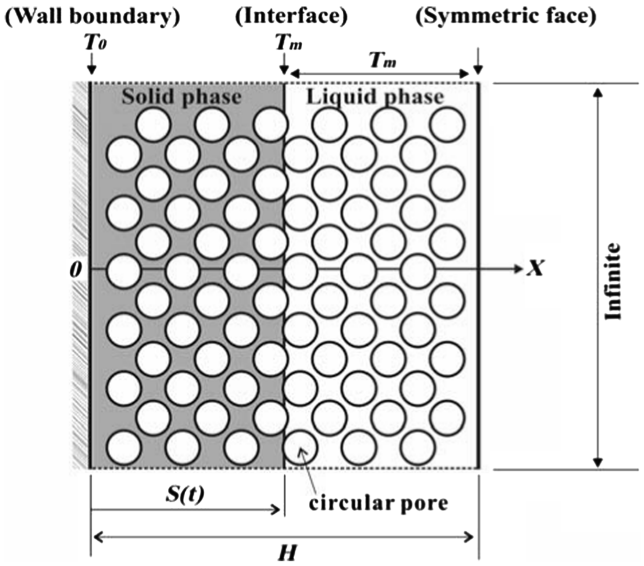

Fig. 1 One-dimensional Stefan problem in a finite region containing two-dimensional low-conducting circular pores.

B. Solidification Interface in a Heterogeneous Medium

Consider next the solidification interface when pores are distributed in a continuous medium. For simplicity, the thermal conductivity, heat capacity, and density of the pores are assumed to be considerably smaller in comparison with those of the continuous medium (both in its liquid and solid phases). With the density of the continuous medium assumed to be independent of temperature, natural convection in the liquid phase is neglected. For the temperature range considered in the present study, the influence of thermal radiation is also neglected. Consequently, heat is transferred only by conduction in the solid and liquid phases.

Thermal conductivity is a key parameter in any heat conduction problem. In the present analysis, the included pores affect the effective thermal conductivity of the heterogeneous medium (mixture of the continuous medium and the pores) and its associated parameters, e.g., the effective thermal diffusivity. For low-conducting pores, the effective thermal conductivity of the porous medium is always smaller than the stagnant thermal conductivity of the continuous medium and dependent upon on the porosity, arrangement, and shape of the pores [11].

A number of analytical models exist for the effective thermal conductivity of a porous medium in steady state [11–14]. In the present study, the well-known Maxwell model for 2-D circular pores periodically distributed in a continuous medium [15] is employed and combined with the Neumann's solutions to solve the solidification problem illustrated in Fig. 1. It should be noted that the 2-D circular pore arrangement is typically anisotropic, varying with its orientation to the nominal direction of conduction. Therefore, the dependence of the effective thermal conductivity on the pore arrangement and the applicability of the 2-D Maxwell model of effective thermal conductivity are both to be numerically validated later.

Following the concept introduced by Maxwell for a spherical pore centered at a cubic continuous medium, the effective thermal conductivity of a continuous medium containing a periodically distributed 2-D circular pore is derived. The relationship between the effective thermal conductivity k_e of the porous medium and that of its composition (thermal conductivity of the continuous medium, k_c) can be expressed as

$$\frac{k_e}{k_c} = \left(\frac{1 + k_p/k_c + \varepsilon(k_p/k_c - 1)}{1 + k_p/k_c + \varepsilon(k_p/k_c + 1)}\right) \tag{4}$$

where k_p is the thermal conductivity of the circular pores, assuming $k_p \ll k_c$ and ε is the porosity. In comparison, the Maxwell model for spherical pores predicts that [15]

$$\frac{k_e}{k_c} = \left(\frac{2 + k_p/k_c - 2\varepsilon(1 - k_p/k_c)}{2 + k_p/k_c + \varepsilon(1 - k_p/k_c)}\right)$$

According to Gibson and Ashby [16], the specific heat, latent heat, and fusion temperature of a porous material are equivalent to those of the dense parent material, and its effective density ρ_e can be written as

$$\rho_e = \rho_c(1 - \varepsilon) + \varepsilon\rho_p \tag{5}$$

where ρ_c and ρ_p are the density of the continuous material and the pores, respectively. Substitution of Eqs. (4) and (5) into the definition of thermal diffusivity, $\alpha = k/\rho c_p$, leads to the following equation for the effective thermal diffusivity α_e for 2-D circular pores:

$$\begin{aligned}\frac{\alpha_e}{\alpha_c} &= f\left(\varepsilon, \frac{k_p}{k_c}, \frac{(c_p)_p}{(c_p)_c}, \frac{\rho_p}{\rho_c}\right) \\ &= \left(\frac{[1 + k_p/k_c + \varepsilon(k_p/k_c - 1)]/[1 + k_p/k_c + \varepsilon(k_p/k_c + 1)]}{(1 - \varepsilon) + \varepsilon([(c_p)_p\rho_p]/[(c_p)_c\rho_c])}\right)\end{aligned} \tag{6}$$

For the solidification of a porous medium, it is assumed that the normalized liquid/solid interface location, ξ of Eq. (1), may be modified to account for the parameters associated with the pore inclusions (e.g., porosity), as

$$\xi = 2\lambda\sqrt{\tau_e} \tag{7}$$

where τ_e is a nondimensional time defined as $\tau_e = \alpha_e t/H^2$. Substitution of Eq. (6) into Eq. (7) yields an analytical solution for the location of solidification interface in the porous medium, as

$$\xi = 2\lambda\sqrt{f\left(\varepsilon, \frac{k_p}{k_c}, \frac{(c_p)_p}{(c_p)_c}, \frac{\rho_p}{\rho_c}\right)\tau} \tag{8}$$

where λ is determined by solving Eq. (2), and

$$f\left(\varepsilon, \frac{k_p}{k_c}, \frac{(c_p)_p}{(c_p)_c}, \frac{\rho_p}{\rho_c}\right)$$

is defined by Eq. (6). It should be noted that the governing equation of the Stefan or Stefan-type problems for a dense material [Eq. (1)] or its extension for a heterogeneous material [Eq. (8)] assumes a sudden step change of the wall temperature at $x = 0$ that remains constant during solidification (i.e., invariant Stefan number).

C. Limitations of the Modified Solution

An analytical model to predict the evolution of the solidification interface in a continuous medium containing periodically distributed low-conducting 2-D circular pores has been derived. To account for the influence of pore inclusions on solidification, the classical Neumann's solution for Stefan problems is coupled with an analytical model of effective thermal properties for porous media. The applicability of the modified analytical solution presented in this study is limited by the assumptions associated with the two fundamental solutions: Neumann's solution and effective thermal-conductivity model. The former is only applicable under Stefan's problem assumptions, including no natural convection (see Zhang et al. [9] for details), and the latter is valid when the selected effective conductivity model properly represents its variation as a function of porosity and topological parameters (e.g., pore shape and arrangement). Therefore, the applicability of the present analytical solution is limited as a result of the combination of both solutions.

III. Experimental Details

A. Test Setup and Samples

In the present study, distilled water is used as a continuous medium that undergoes solidification, and long circular cylindrical acrylic tubes (length/outer diameter of 25, with tube inner and outer diameters equal to 4 and 2 mm, respectively) serving as 2-D low-conducting pores are periodically distributed in the distilled water. Figure 2 schematically shows the test rig purposely designed and fabricated for the present study.

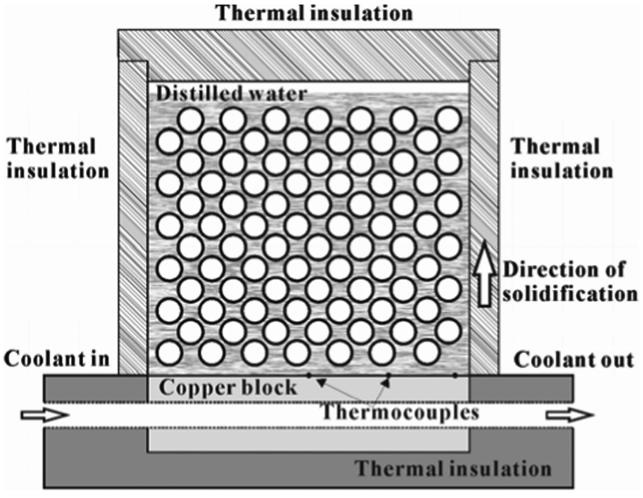

Fig. 2 Schematic of test rig used in the present solidification study.

In the experiment, distilled water in a cubic container with the size of 0.1 m (width) by 0.1 m (depth) by 0.1 m (height) was frozen (solidified). The walls of the container (except the bottom wall) were made of 0.03-m-thick acrylic plate, with a 0.03-m-thick thermal insulation foam attached to each wall (excluding for a monitoring window). Heat was removed from the bottom of the test cube made of a 0.01-m-thick copper plate. Coolant from a refrigerator (Contraves Rheotherm 115) flows through wound passages machined into the copper plate. Three T-type thermocouples were placed on the surface of the copper plate to monitor changes of the plate temperature $T_0(t)$ during the process of solidification. The thermocouples were then connected to a temperature scanner (Agilent).

In each tube, air was sealed tight to reduce the effective thermal conductivity of the tube (pore). The thermal-conductivity ratio of solidified (frozen) distilled water (i.e., ice k_c to cylinder tubes k_p) was estimated to be approximately $k_c/k_p = 13.3$. Two test samples were fabricated, with one having inline arrangement of the circular pores and the other having staggered pore arrangement. The porosity and pitches S_1 and S_2 between the neighboring cylinder elements of the samples are fixed to be $\varepsilon = 0.5$, $S_1 = 5$ mm, and $S_2 = 7.07$ mm, respectively (Fig. 3).

B. Image Processing for Solidification Interface Location

Images of the solidification interface, i.e., boundary between ice being formed and distilled water, were recorded through an observing window of the test rig. Based on the still images continuously captured, the location of the solidification interface was calculated. Each captured image in the red–green–blue plane was converted into the hue–saturation–intensity plane using a commercially available program. Because the liquid and solid phases have distinctively different intensity values, the interface can be determined for a selected time frame.

IV. Numerical Simulations for the Effects of Porosity and Pore Arrangement

Steady-state conduction in the two-phase porous medium with periodically distributed 2-D circular pores was numerically simulated using a commercial program (FLUENT) to validate the applicability of the 2-D Maxwell effective thermal-conductivity model. The calculation domain is illustrated in Fig. 4. Constant heat flux ($q'' = 3000$ Wm^{-1} K^{-1}) was imposed at $x = 0$ and the other end of the two-phase medium, $x = L$, was subjected to natural convection cooling with a prescribed heat transfer coefficient of $h_{nc} =$ 5 Wm^{-2} K^{-1}. The side faces of the computational domain were set to be symmetric. The interface between the circular pores and continuous medium was treated to be adiabatic, as the analytical solution assumes a large thermal-conductivity ratio of the two phases. The physical parameters used for the present simulations are $L_x = 0.16$ m, $L_y = 0.015$ m, $S_1 = 0.015$ m, $S_2 = 0.0212$ m, and $k_c = 15$ Wm^{-1} K^{-1}. To vary the porosity, the diameter of each circular pore (element) was varied and the distances (pitches) between the neighboring pores, S_1 and S_2, remained unchanged.

Unlike isotropic porous media (e.g., open- or closed-cell foams), the effective thermal conductivity of the present porous medium varies according to the orientation of the periodically distributed circular pores relative to the nominal direction of conduction. To examine this aspect, with the porosity fixed, the inline arrangement of the circular pores (Fig. 3a) was systematically rotated, eventually

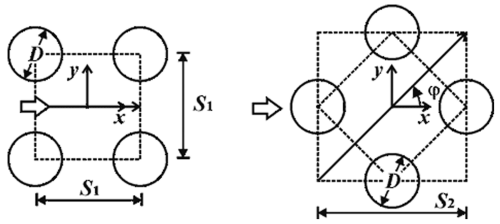

Fig. 3 Unit cell configuration of cylinder arrangement: a) inline arrangement ($\varphi = 0°$) and b) staggered arrangement ($\varphi = 45°$).

leading to the staggered arrangement (Fig. 3b), where the yaw angle φ of 0° denotes the inline arrangement. Topologically, this configuration has a $\pi/4$ period.

V. Discussion of Results

A. Evolution of Solidification Interface in a Continuous (Homogeneous) Material

Consider a continuous medium ($\varepsilon = 0$), initially in liquid phase at T_m. First, at $t = 0$ (i.e., $t = 0$), the wall temperature at $x = 0$ is instantly dropped to a constant temperature $T_0 (< T_m)$. In this case, the Stefan number is invariant in time. As a result, solidification initiates from a region in the immediate vicinity of the wall boundary, $x = 0$. As time elapses, the solid phase gradually thickens. Figure 5 shows how the location of the solid/liquid interface (i.e., solidification interface) varies with time. In comparison, Fig. 5 also exhibits the experimental data.

Qualitatively, the nonlinear trend common for all the data shown in Fig. 5 is attributed to the fact that the solidification front moves slower as it moves away from the wall boundary $x = 0$. The conduction of heat in the solidified layer is governed by Fourier's law, as

$$q'' = -k(T_0 - T_m)/S(t) \tag{9}$$

For a given temperature difference (i.e., $T_0 - T_m$ or a constant Stefan number) and with the assumption of invariant thermal conductivity, the solidification interface moves away from the wall boundary ($x = 0$) as time elapses. Therefore, the effective heat flux q'' traveling though the solidified layer decreases in a nonlinear manner as $q'' \sim 1/S(t)$. This causes the deceleration of the solidification rate as the solid/liquid interface moves away from the wall boundary.

Quantitatively, the analytical model (1) overpredicts the solidification interface location obtained from the present experiments (e.g., 14.8% overestimation at $\tau = 2.5$). It should be noted that the analytical solutions for Stefan or Stefan-type problems assume that there is a sudden step change of the thermal boundary condition (e.g., constant temperature T_0 imposed at the boundary surface $x = 0$). Such an idealized thermal boundary is hardly achieved in reality. As shown in Fig. 6, the experimentally measured wall temperature drops rapidly with time, followed by a gradual approach to the prescribed wall temperature T_0, and the deviation of the measured wall temperature from the idealized one decreases as the solidification progresses. This may explain the observed discrepancy between the analytical solution of Eq. (1) and the experimental data in Fig. 5. To confirm this, numerical simulation results taking into consideration the actual wall-temperature profile (Fig. 6) are included in Fig. 5 for comparison. Excellent agreement between the data obtained from the present numerical simulation and the experiment clearly indicates that the actual nonstep change of the wall temperature causes the delay of solidification as observed in Fig. 5.

It should be noted that although numerous efforts have been made to analytically take account for the real wall-temperature variation in time (e.g., Fig. 6), at present, such analytical solutions have not been reported (including this study), due to mathematical complexities of multidimensional transient heat transfer with a moving boundary. The present study assumes that a systematic discrepancy exists between the analytical solution [Neumann's solution, Eq. (1)] and the experimental data, due to different wall boundary conditions for a given test setup with/without the 2-D pore inclusions.

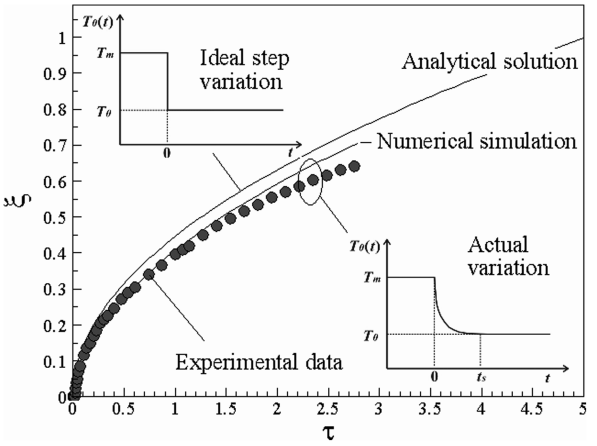

Fig. 5 Temporal evolution of solidification interface (ξ) in a continuous medium (distilled water).

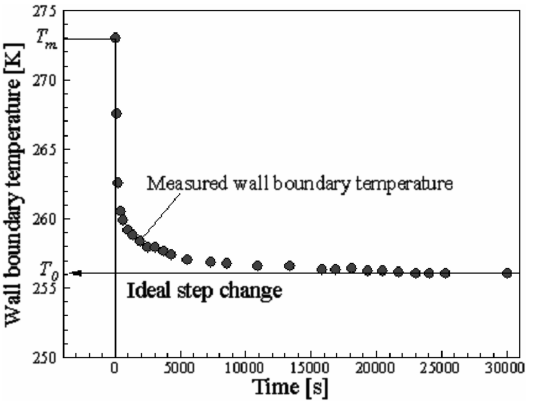

Fig. 6 Variation of wall boundary temperature T_0 at $x = 0$ with time.

B. Effective Thermal Conductivity with Two-Dimensional Pore Inclusions

Because the present analysis of solidification in a continuous medium containing low-conducting 2-D circular pores assumes that the pore inclusions act to mainly influence the effective conductivity of the porous medium, the selection of a fundamental effective conductivity model is crucial. Kaviany [17] pointed out that the generalization of fundamental effective conductivity models based on the porosity and conductivity ratio of the two phases alone is not feasible, as detailed topological information (e.g., shape factor) is also important. As previously mentioned, the 2-D Maxwell model is employed in the present analysis among other fundamental models. Before proceeding further, it is essential to justify the applicability of the Maxwell model for the present configuration.

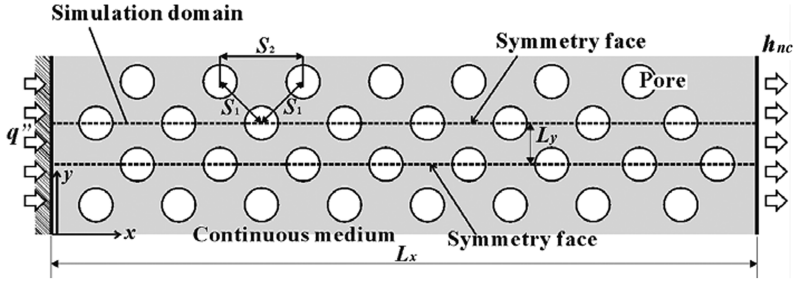

Fig. 4 Calculation domain for steady conduction in continuous medium with two-dimensional circular pores (showing staggered arrangement, $\varphi = 45°$).

Figure 7 plots the effective thermal conductivity normalized by the stagnant thermal conductivity of the continuous medium (k_e/k_c) as a function of porosity. The assumption of a large thermal-conductivity ratio between the continuous medium and pores (i.e., $k_c \gg k_p$) simplifies the problem. Data from some fundamental models [18] are also included.

It is common among all the models, including the present numerical simulations, that the increase in the porosity causes a monotonic decrease in the effective thermal conductivity. It is known that if conduction is the only mechanism of heat transfer in the porous medium, the series model (not included) and the parallel model set the lower and upper bounds for the effective conductivity, respectively. It is seen from Fig. 7 that, in general, the data points obtained from the present calculation follow the 2-D Maxwell model well. On the other hand, at high porosity levels, the 2-D Maxwell model appears to slightly overpredict the effective thermal conductivity. For a further confirmation, a set of data reported by Fiedler et al. [19], who numerically calculated the effective thermal conductivity of 2-D and 3-D porous media (including 2-D cylinder banks identical to that considered in this study), is plotted together in Fig. 7. Good agreement with the present calculation within the porosity range considered is achieved, validating the Maxwell conductivity model employed in the present configurations.

C. Evolution of Solidification Interface in a Heterogeneous Medium

To examine the influence of periodically distributed 2-D circular pores in a continuous medium (distilled water, both liquid and solid phases) on its overall solidification behavior, a selected porosity case, $\varepsilon = 0.5$, for the unit cell configuration illustrated in Fig. 3 is next considered.

Figure 8 presents the snapshots of the solidification interface at selected nondimensional solidification time: $\tau = 0.26$, 0.85, 1.87, and 2.77 for the staggered arrangement. When the solidification interface (an isothermal line) passes the pores placed in the continuous medium, it is locally expected to be posed almost perpendicular to the circumference of the circular pores at any given time, due to significantly low thermal conductivity of the circular pores. Since many circular pores are transversely placed, the solidification interface tends to exhibit a transversely wavy pattern. However, this feature is not clearly visible from Fig. 8. During the image processing, the location of the solid/liquid interface in which the least interference from the transverse pores was present was chosen as the representative location ξ of the solidification interface. The representative location of the solidification interface from selected images (including those displayed in Fig. 8) is shown in Fig. 9.

It is seen from Fig. 9 that the nonlinear and monotonic evolution of the solidification interface with time follows the same trend as that of the continuous medium in Fig. 5, although the presence of pores in the continuous medium significantly delays the solidification. Furthermore, the experimental data obtained from the inline

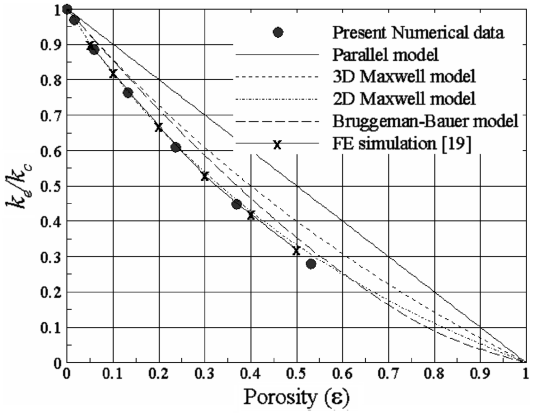

Fig. 7 Comparison of numerically calculated effective thermal conductivity with those predicted by fundamental models as a function of porosity.

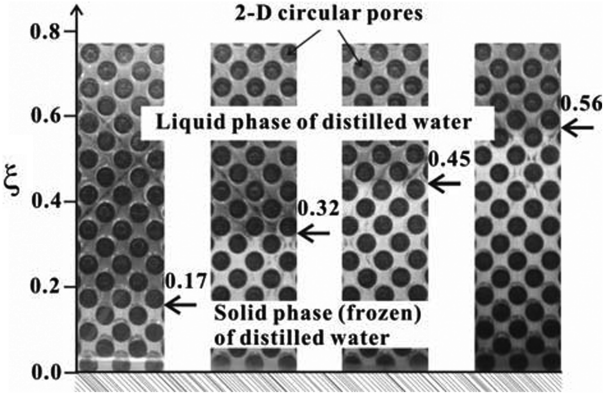

Fig. 8 Snapshots of solidification interface of distilled water containing periodically distributed 2-D circular pores in staggered arrangement at selected nondimensional solidification time: a) $\tau = 0.26$, b) $\tau = 0.85$, c) $\tau = 1.87$, and d) $\tau = 2.77$.

arrangement of the circular pores show faster evolution of the solidification interface than that from the staggered arrangement, although the porosity is fixed, and the predicted evolution of the solidification interface in the continuous medium with 2-D circular pores underestimates the experimental data of both pore configurations (for k_p of acrylic and air). For example, at $\tau = 2.5$, an underestimation of 9.2% (staggered) and 13.4% (inline) of solidification is observed from Fig. 9. In comparison, approximately 14.8% was overpredicted by the analytical solution for the continuous material at $\tau = 2.5$ (Fig. 5). On the other hand, assuming nonconducting pores (i.e., $k_p = 0$) is shown to overestimate the solidification interface location [e.g., 11.7% (staggered) and 6.8% (inline) at $\tau = 2.5$]. The further delay of solidification in the staggered arrangement suggests that the effective thermal conductivity of this arrangement is lower than that of the inline arrangement (to be discussed later).

In summary, the retardation of solidification can be explained by the reduction of effective thermal conductivity and diffusivity due to the presence of low-conducting pores. For example, the effective thermal conductivity drops down to roughly 33% of that of the continuous material if $\varepsilon = 0.5$. Correspondingly, the solidification front only reaches about 67% of the total thickness of the continuous medium by the time the continuous medium is fully solidified. The comparison (from the analytical models) showing good agreement at least in a qualitative manner suggests that the main mechanism of the retarded solidification is the reduced effective conductivity and diffusivity due to pore inclusions, since it is taken in the analytical solution as the sole controlling factor.

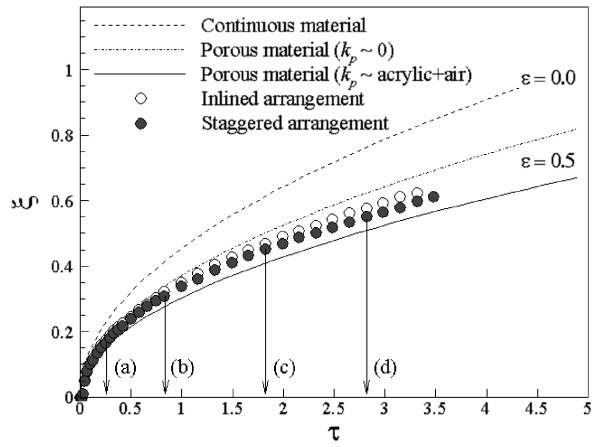

Fig. 9 Temporal evolution of solidification interface (ξ) in a continuous medium (distilled water) containing periodically distributed 2-D circular pores in both inline and staggered arrangements; analytical prediction with ideal step wall-temperature drop (lines) and experimental data (circles).

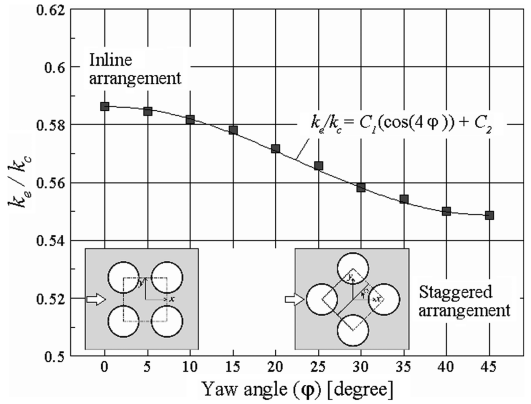

Fig. 10 Numerically predicted effective thermal conductivity plotted as a function of orientation (yaw) angle of 2-D circular pores ($\varepsilon = 0.245$).

D. Effect of Pore Arrangement on Solidification Interface

It has been shown that even for a given porosity and pore shape (circular), the solidification interface evolves in a different manner when the pore arrangement is changed. It can be inferred from Fig. 9 that the inline arrangement has a higher effective thermal conductivity than that of the staggered arrangement. To elaborate the anisotropic effective conductivity tensor in the periodically distributed pore arrangement, another set of numerical simulations was conducted. To simplify the problem, only four cylindrical pore elements shown in the inset of Fig. 10 were considered. As a result, the value of the effective thermal conductivity obtained at $\varepsilon = 0.245$ was approximately 8% lower than that of the multipore case (Fig. 4).

Figure 10 plots the calculated effective thermal conductivity as a function of yaw angle from $\varphi = 0°$ (inline) to $\varphi = 45°$ (staggered), with the porosity fixed at $\varepsilon = 0.245$. Upon increasing the yaw angle from the inline to the staggered arrangement, the effective conductivity is monotonically decreased. The effective conductivity of the latter arrangement was found to be 6.5% lower than that of the former. The variation of the effective conductivity with the yaw angle may be correlated as

$$k_e/k_c = C_1(\cos(4\varphi)) + C_2 \tag{10}$$

where

$$C_1 = (k_e/k_c)_{\max} - (k_e/k_c)_{\min}$$

and

$$C_2 = ((k_e/k_c)_{\max} + (k_e/k_c)_{\min})/2$$

This correlation suggests that as the bank of the circular pores becomes increasingly staggered (i.e., the yaw angle is increased), the thermal flow passage becomes more tortuous (as also pointed out by Olives and Mauran [20]), leading to the further reduction of the effective conductivity. Correspondingly, the solidification is retarded further, as observed in Fig. 9 for a given porosity.

VI. Conclusions

An analytical model to predict the evolution of solidification interface in a continuous medium containing periodically distributed low-conducting 2-D circular pores is presented. The classical solidification model (Neumann's solution for Stefan problems) is coupled with an analytical model of effective thermal conductivity for porous media to account for the influence of the pore inclusions on solidification. The effects of different wall thermal boundary conditions and pore arrangements on the overall solidification behavior of the porous medium are also considered. The applicability of the model predictions is examined by comparing with experimental measurements (solidification of distilled water with and without low-conducting circular pores). Good agreement between analytical predictions and experimental results (with a systematic deviation) suggests that the effective thermal conductivity plays a major role in the solidification of a porous medium. As the porosity is increased, the full solidification of the medium is further delayed due to the reduced effective conductivity. The analytical model presented, which is simple and expressed in closed form, can shed light on how the inclusion of low-conducting pores reduces the effective thermal conductivity of a porous medium and delays its full solidification.

Acknowledgments

This work is supported by the National Basic Research Program of China (2006CB601203), the National Natural Science Foundation of China (50676075, 10632060, 10825210), the National 111 Project of China (B06024), and the National High Technology Research and Development Program of China (2006AA03Z519).

References

[1] Flemings, M. C., *Solidification Processing*, McGraw–Hill, New York, 1974.

[2] Muehlbauer, J. C., and Sunderland, J. E., "Heat Conduction with Freezing or Melting," *Applied Mechanics Reviews*, Vol. 18, No. 12, 1965, pp. 951–957.

[3] Zalba, B., Marin, J. M., Cabeza, L. F., and Mehling, H., "Review on Thermal Energy Storage with Phase Change: Materials, Heat Transfer Analysis and Applications," *Applied Thermal Engineering*, Vol. 23, No. 3, 2003, pp. 251–283. doi:10.1016/S1359-4311(02)00192-8

[4] Stefan, J., "Uber die Throrie der Eisbildung, Insbesondereuber die Eisbildung in Polarmaere," *Annalen der Physik und Chemie*, Vol. 278, No. 2, 1891, pp. 269–286. doi:10.1002/andp.18912780206

[5] Carslaw, H. S., and Jaeger, J. C., *Conduction of Heat in Solids*, Oxford Univ. Press, Oxford, 1959.

[6] Goodman, T. R., "The Heat Balance Integral and Its Applications to Problems Involving Change of Phase," *Journal of Heat Transfer*, Vol. 80, No. 3, 1958, pp. 335–341.

[7] Lightfoot, N. M. H., "The Solidification of Molten Steel," *Proceedings of the London Mathematical Society*, Vol. 31, No. 2, 1929, pp. 97–116.

[8] Pedroso, R. I., and Domoto, G. A., "Inward Spherical Solidification-Solution by the Method of Strained Coordinates," *International Journal of Heat and Mass Transfer*, Vol. 16, 1973, pp. 1037–1043. doi:10.1016/0017-9310(73)90042-2

[9] Zhang, B., Kim, T., and Lu, T. J., "Analytical Solution for Solidification of Close-Celled Metal Foams," *International Journal of Heat and Mass Transfer*, Vol. 52, No. 1, 2009, pp. 133–141. doi:10.1016/j.ijheatmasstransfer.2008.06.006

[10] Zhang, B., Kim, T., and Lu, T. J., "The Solidification of Two-Phase Heterogeneous Materials: Theory Versus Experiment," *Science in China, Series E (Technological Sciences)*, Vol. 52, No. 6, 2009, pp. 1688–1697. doi:10.1007/s11431-008-0327-y

[11] Bauer, T. H., "A General Analytical Approach Toward the Thermal Conductivity of Porous Media," *International Journal of Heat and Mass Transfer*, Vol. 36, No. 17, 1993, pp. 4181–4191. doi:10.1016/0017-9310(93)90080-P

[12] Russell, H. W., "Principles of Heat Flow in Porous Insulators," *Journal of the American Ceramic Society*, Vol. 18, No. 1, 1935, pp. 1–5. doi:10.1111/j.1151-2916.1935.tb19340.x

[13] Loeb, A. L., "Thermal Conductivity VIII: A Theory of Thermal Conductivity of Porous Materials," *Journal of the American Ceramic Society*, Vol. 37, No. 2, 1954, pp. 96–99.

[14] Wang, J. F., Carson, J. K., North, M. F., and Cleland, D. J., "A New Approach to Modelling the Effective Thermal Conductivity of Heterogeneous Materials," *International Journal of Heat and Mass Transfer*, Vol. 49, No. 17, 2006, pp. 3075–3083. doi:10.1016/j.ijheatmasstransfer.2006.02.007

[15] Maxwell, J. C., *A Treatise on Elasticity and Magnetism*, 3rd ed., Clarendon Press, Oxford, 1892.

[16] Gibson, L. J., and Ashby, M. F., *Cellular Solids: Structure and Properties*, 2nd ed., Cambridge Univ. Press, New York, 1997.

[17] Kaviany, M., *Principles of Heat Transfer in Porous Media*, Springer–Verlag, New York, 1991.

[18] Solórzano, E., Reglero, J. A., Rodríguez-Pérez, M. A., Lehmhus, D., Wichmann, M., and De Saja, J. A., "An Experimental Study on the Thermal Conductivity of Aluminium Foams by Using the Transient

Plane Source Method," *International Journal of Heat and Mass Transfer*, Vol. 51, No. 25–26, 2008, pp. 6259–6267. doi:10.1016/j.ijheatmasstransfer.2007.11.062

[19] Fiedler, T., Pesetskaya, E., Öchsner, A., and Grácio, J., "Calculations of the Thermal Conductivity of Porous Materials," *Materials Science Forum*, Vols. 514–516, Pt. 1, 2006, pp. 754–758. doi:10.4028/www.scientific.net/MSF.514-516.754

[20] Olives, R., and Mauran, S., "A Highly Conductive Porous Medium for Solid-Gas Reactions: Effect of the Dispersed Phase on the Thermal Tortuosity," *Transport in Porous Media*, Vol. 43, 2001, pp. 377–394. doi:10.1023/A:1010780623891